

RESEARCH AND EDUCATION

Numeric simulation of occlusal interferences in molars restored with ultrathin occlusal veneers



Pascal Magne, DMD, MS, PhD<sup>a</sup> and Raymond Cheung, MS<sup>b</sup>

Over time, occlusal enamel may be worn down or severely eroded, reducing its thickness and even exposing the underlying dentin at the occlusal surface.<sup>1</sup> In such situations, thin or ultrathin bonded posterior occlusal veneers are a conservative alternative to traditional onlays or complete crown coverage.<sup>2-5</sup>

Materials used for ultrathin (0.6-mm) bonded posterior occlusal veneers must be durable and used in combination with the immediate dentin bonding technique.<sup>2</sup> Computer-aided design and computer-aided manufacturing (CAD-CAM) technology allows the restoration to be fabricated from composite resins or ceramic blocks, including Paradigm MZ100 (3M ESPE) composite resin and e.max CAD (Ivoclar Vivadent AG) glass ceramic.<sup>3,6-9</sup> Although either of these materials can be used, material selection requires an understanding of how stresses are distributed during functional and parafunctional forces. Excursive interferences and parafunction may induce premature breakdown<sup>10</sup> and must also be considered.

The finite element method allows visual demonstration of the effect of occlusion on stress distribution in

ABSTRACT

**Statement of problem.** Selecting material for a minimally invasive occlusal veneer reconstruction concept requires an understanding of how stresses are distributed during functional and parafunctional forces.

**Purpose.** The purpose of this in vitro study was to investigate stress distribution in a maxillary molar restored with ultrathin occlusal veneers and subjected by an antagonistic mandibular molar to clenching and working and nonworking movements.

**Material and Methods.** A maxillary first molar was modeled from microcomputed tomography (micro-CT) data, using medical image processing software, stereolithography editing/optimizing software, and finite element software. Simulated ultrathin occlusal veneer materials were used. The mandibular molar antagonist was a solid nondeformable geometric entity. Loads simulated clenching, working, and nonworking movements with loading of 500 N. The values of the maximum principal stress were recorded.

**Results.** In the clenching load situation, maximum tensile stresses were located at the occlusal veneer (52 MPa for composite resin versus 47 MPa for ceramic). In the working movement, significant additional tensile stresses were found on the palatal root (87 MPa for composite resin and 85 MPa for ceramic). In the nonworking movement, tensile stress on the ultrathin occlusal veneer increased to 118 MPa for composite resin and 143 MPa for ceramic veneers. Tensile stress peaks shifted to the mesiobuccal root (75 MPa for composite resin and 74 MPa for ceramic).

**Conclusions.** The topography of stresses generated by the various occlusal interferences were clearly identified. Significant tensile stress concentrations were found within the restoration's occlusal topography and root, with the nonworking interference being the most harmful and also the most revealing of the difference between the composite resin and ceramic ultrathin occlusal veneers. (*J Prosthet Dent* 2017;117:132-137)

teeth.<sup>11</sup> In a previous study,<sup>12</sup> the finite element method was used to model an ultrathin bonded posterior occlusal veneer under vertical loading with a geometric sphere as an antagonist. The results demonstrated that both CAD-CAM composite resin and ceramic materials can be satisfactory materials.<sup>12,13</sup>

This study is an extension of previous studies and investigated tensile stress peaks on a maxillary first molar

Supported by MSC Software Corp and Materialise Co.

<sup>a</sup>The Don and Sybil Harrington Professor of Esthetic Dentistry, Department of Restorative Sciences, Herman Ostrow School of Dentistry of the University of Southern California, Los Angeles, Calif.

<sup>b</sup>Doctoral student, Herman Ostrow School of Dentistry of the University of Southern California, Los Angeles, Calif.

## Clinical Implications

Excursive interferences generate the highest tensile stresses in occlusal restorations and should be avoided by careful occlusal adjustments or by providing canine guidance.

with an ultrathin composite resin and ceramic occlusal veneer. Various 3-dimensional finite element models of a restored tooth were subjected by the antagonistic mandibular first molar in simulated loading to clenching (MIP), working, and nonworking movements. The 2 null hypotheses were that no differences would be found in stress distribution with an ultrathin bonded posterior occlusal veneer based on material selection (composite resin versus ceramic) and that no differences would be found in stress distribution based on loading (MIP, working, and nonworking).

## MATERIAL AND METHODS

Three-dimensional finite element models were created from an extracted human left maxillary first molar and left mandibular first molar by using previously validated protocols.<sup>13</sup> The teeth were digitized as a raw set of micro-computed tomography slices with a voxel dimension of 13.67  $\mu\text{m}$ . The individual slices were then processed with medical image processing software (Mimics; Materialise), which converted the 2-dimensional images into a 3-dimensional model. For the maxillary tooth, masks were created based on image density to separate and identify enamel and dentin portions of the tooth. The pulp chamber and root canals were generated as an empty space. For both maxillary and mandibular teeth, the 3-dimensional models were then saved as stereolithography files, and the Remesh functionality in Mimic software was used to reduce the number of triangles for finite element modeling and to improve the overall quality of the mesh (such as adapting the triangle density to the complexity of the geometry). The stereolithography files were then further manipulated with software (3-Matic; Materialise), which refined the mesh, allowing congruency of the elements used for the interface of the dentin and enamel meshes. When the dentin model was viewed in cross-section, unwanted surfaces in the pulp chamber were deleted. Within 3-Matic software, the dentin-enamel model was split using intersection parts to simulate an occlusal reduction and the 0.6-mm-thick occlusal veneer. A geometric cylinder was generated and modified by subtractive intersection with the root to act as the surrounding bone. Again, the new meshes were refined to allow for congruency of elements at the various interfaces. A continuous mesh was

**Table 1.** Material properties

Property	Composite Resin Occlusal Veneer	Ceramic Occlusal Veneer	Dentin	Enamel	Bone
Young modulus (GPa)	16	95	18.6	84.1	14.7
Poisson ratio	0.24	0.30	0.31	0.30	0.30

achieved, which could be verified by a quality control tool built into 3-Matic.

The exported files were imported as finite element models into software (Marc/Mentat; MSC Software). Finite element volumetric meshes were created. Material properties were then assigned to the respective part of the assembly. The 2 ultrathin occlusal veneer materials were Paradigm MZ100 (3M ESPE), used for the ultrathin composite resin occlusal veneer, and e.max CAD (Ivoclar Vivadent AG), used for the ultrathin ceramic occlusal veneer. Table 1 shows the material properties used in this study. Figure 1 shows the model assembly in an expanded view displaying each individual material component. The mandibular molar antagonist was a solid nondeformable geometric entity.

Fixed boundary conditions were applied at the bottom of the stone base. The 3 load situations were created to represent the mandibular movements of clenching (vertical, upward), working (horizontal, left), and nonworking interferences (horizontal, right). For all load situations, the starting occlusal position of the mandibular antagonist to the maxillary molar was close to MIP. A force of 500 N was chosen for each load situation as it represented a force slightly lower than the maximum that can be generated by women.<sup>14</sup> For clenching, a vertical force was directed from the antagonist up into the maxillary molar. Three contacts were made on the mesial marginal ridge, oblique ridge, and distal lingual cusp. For the working and nonworking movements, the lateral forces were directed to their respective sides from the antagonist mandibular molar. For the working movement, 2 contacts were made at the mesiobuccal and distobuccal cusps of the maxillary molar. For the nonworking movement, contact was made only on the mesiolingual cusp. The load situations were submitted to the Marc software, and an output file was generated for postprocessing and analysis. Information about the maximum principal value of stress was recorded as color maps with positive values representing tensile stresses. Peak tensile stresses were recorded numerically.

## RESULTS

In the clenching load situation, tensile stress concentrations were found at the mesial aspect of the ultrathin occlusal veneer and below the mesial marginal ridge in enamel. Tensile stress formation was mild along the

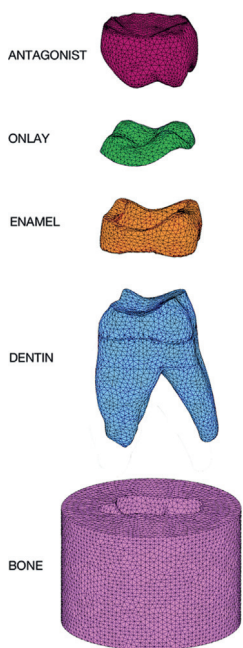


Figure 1. Material components of simulation model.

central development groove. The maximum tensile stress on the ultrathin occlusal surface was similar for both materials at 52 MPa for composite resin versus 47 MPa for ceramic (Table 2). The maximum tensile stress for ceramic was 11% lower than that of composite resin. Similarly, the tensile stress in enamel under the mesial marginal ridge was 38 MPa and 31 MPa, respectively. The roots were essentially under compression, especially at the root trunk, and exhibited a negligible amount of tensile stress at 1 MPa. The distribution of stresses along the buccal and lingual grooves of the ultrathin occlusal veneer was different as seen in the color map distribution in Figure 2.

In the working movement for both materials, lateral contact was along both buccal cusps. Higher tensile stresses concentrated around the central developmental groove and slightly along the buccal groove. The buccal groove also had lower tensile stress in the ultrathin composite occlusal veneer. Functional lateral movement caused both of the buccal roots to be under compression and the palatal root to be under tension. The maximum tensile stress recorded for the ultrathin ceramic occlusal veneer highlighted the difference in material with 54 MPa on the center of the oblique ridge, whereas for the ultrathin composite resin occlusal veneer, it was 44 MPa. The maximum tensile stress for ceramic was 23% higher than that of composite resin. Both of the materials, however, exhibited similar levels of tensile stress on the palatal root with 87 MPa for composite resin and 85 MPa for ceramic.

In the nonworking movement for both of the materials, lateral contact was only along the mesial lingual

Table 2. Maximum principal value of stress for three load situations

Location	Composite Resin (MPa)	Ceramic (MPa)
Clenching load situation		
Occlusal veneer	52	47
Enamel (under marginal ridge)	38	31
Root	1	1
Working load situation		
Occlusal veneer (central groove)	44	54
Root (palatal)	87	85
Nonworking load situation		
Occlusal veneer (mesiolingual cusp)	118	143
Root (mesiobuccal)	75	74

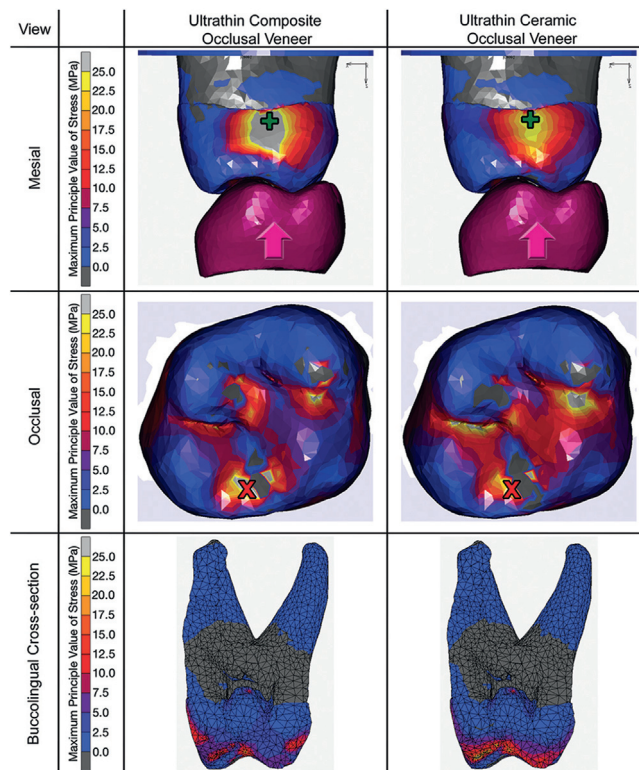


Figure 2. Results of clenching load situation. Output file was postprocessed to record maximum principal value of stress located on veneer and root for each material. Highest value on tooth indicated with a green plus sign and on occlusal veneer with red X.

cusps. Tensile stresses were pronounced as they wrapped around a single cusp along the central developmental groove, across the oblique ridge, and through the lingual groove. Parafunctional lateral movement caused the palatal root to be under compression and both of the buccal roots to be under tension. The maximum tensile stress recorded for the ultrathin ceramic occlusal veneer highlighted the difference in material with 143 MPa on the mesial lingual cusp, whereas for the ultrathin composite resin veneer, it was 118 MPa. The maximum tensile stress for ceramic was 21% higher than that of

composite resin. Both of the materials, however, exhibited similar levels of tensile stress on the mesio-buccal root with 75 MPa for composite resin and 74 MPa for ceramic.

**DISCUSSION**

This research examined 3 different load scenarios and 2 material selections for ultrathin occlusal veneers in the posterior dentition. The first null hypothesis was rejected because a difference was found in the stress distribution of the ultrathin occlusal veneer based on material selection. The second null hypothesis was also rejected because of the significant difference in stress based on load situations in both the ultrathin occlusal veneer and tooth.

This study's results are based on the finite element method. An advantage of using this method is the visual and numerical demonstration of tensile stress in a tooth and restoration which would otherwise not be possible. The accuracy of the computer simulation is defined by the number of elements and geometry of the elements used for mathematical approximations of tensile stress. This model simulated a worst-case scenario of clenching and laterotrusive interferences lacking anterior guidance. It also simulated perfectly bonded interfaces between tooth and restoration. Clinically, this correlates with ideal enamel bonding and the use of optimized dentin bonding procedures such as immediate dentin sealing,<sup>15</sup> as well as appropriate conditioning and bonding to the machined restorative materials (airborne-particle abrasion and the use of a silane for the composite resin, hydrofluoric etching and use of a silane for the ceramic). The material properties of the antagonist mandibular molar were simplified as it was given an infinite modulus of elasticity by modeling it as a nondeformable rigid body.

In the clenching load situation, tensile stress concentrated on the ultrathin occlusal veneer and below the mesial marginal ridge, representing horizontal expansion of the enamel periphery under a vertical compressive load. Due to the decreased material stiffness of MZ100 compared with that of e.max CAD, the mesiolingual and mesiobuccal cusps had greater deflection for the ultrathin MZ100 occlusal veneer. Although tensile stress was greater below the mesial marginal ridge for the ultrathin MZ100 occlusal veneer, the magnitude of the tensile stress was inferior (31 to 38 MPa) to that of the ultrathin occlusal veneer (47 to 52 MPa). This load situation illustrated that more destructive tensile stress from clenching concentrates within the veneer itself rather than the tooth, which is well designed to handle clenching forces. The main difference between materials was the distribution of stress along the buccal and lingual grooves of the ultrathin occlusal veneer, which were

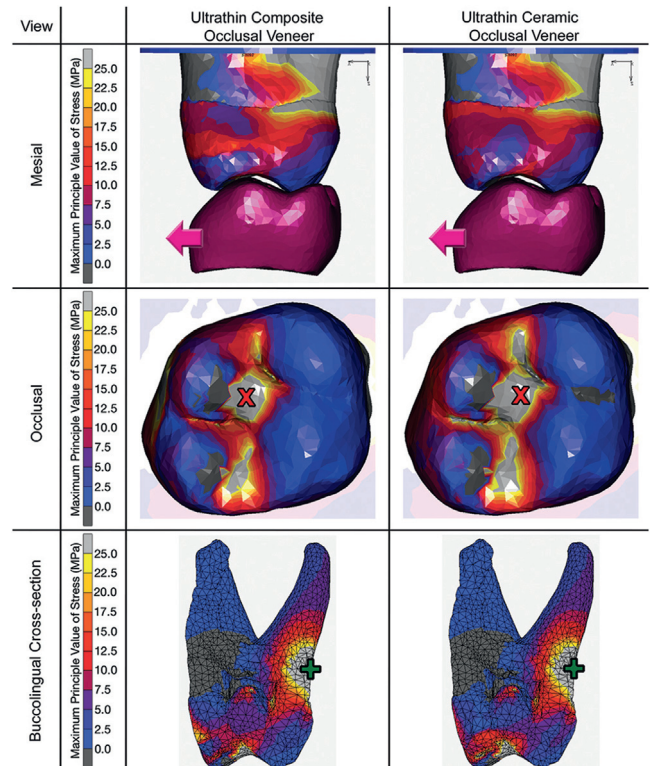


**Figure 3.** Results of working load situation. Output file was postprocessed to record maximum principal value of stress located on veneer and root for each material. Highest value on tooth indicated with a green plus sign and on occlusal veneer with red X.

higher for the ceramic (Fig. 2). This formation was due to the rigidity of the ceramic and resistance to deformation, directing tensile stress into areas of sharp concavity (deep grooves) on the occlusal veneer. This finding is in agreement with existing data showing the increased crack propensity of e.max CAD compared with that of MZ100 during accelerated fatigue testing.<sup>2,3</sup> From this load situation, the compressive force at the root trunk (buccolingual cross-section in Fig. 2) for both materials made catastrophic failure of the tooth (root fracture) induced by clenching unlikely. This same conclusion was reached in a previous study with a 2-dimensional simulation, where clenching compressive forces were found to dominate the entire coronal volume<sup>16</sup> but in which root and periodontal structures were not modeled. Hence, the 3-dimensional model of the present study is more comprehensive and demonstrates the critical role of the root trunk in protecting posterior teeth from catastrophic fracture under clenching conditions.

MZ100 shows stress concentration that is decreased compared with that of e.max CAD for working and nonworking movements. In the working load situation, both buccal cusps were deflected by contact, explaining the tensile stresses along the central groove from mesial to distal, with e.max CAD occlusal veneer exhibiting higher

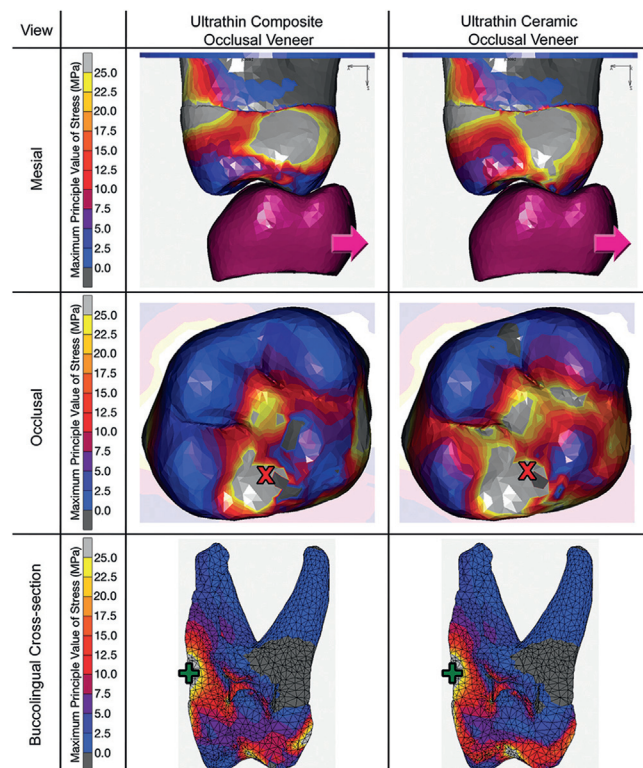


**Figure 4.** Results of nonworking load situation. Output file was postprocessed to record maximum principal value of stress located on veneer and root for each material. Highest value on tooth indicated with a green plus sign and on occlusal veneer with red X.

stress values. In the nonworking movement, only the mesiolingual cusp was deflected by contact and induced tensile stress mainly in grooves adjacent to that cusp. Here again, the ultrathin ceramic occlusal veneer exhibited higher values of stress, especially pronounced across the oblique ridge through the lingual and buccal groove as shown in Figure 4 (occlusal view). In both the working and the nonworking load situations, maximum tensile stress on the ultrathin occlusal veneer for the e.max CAD increased by over 20% compared with MZ100. In these load situations, the ultrathin e.max CAD occlusal veneer exhibited more tensile stress accumulation distributed within the veneer itself than in the ultrathin MZ100 occlusal veneer as shown in the buccolingual cross-section of Figures 3 and 4.

Restoration thicknesses for composite resin and ceramic veneers ranging from ultrathin to thin have been shown in vitro to be a viable definitive posterior restoration.<sup>2-5</sup>

A standard thickness occlusal veneer has an occlusal reduction of 2 mm, 1 mm for thin and 0.6 mm for ultrathin. For both the working and the nonworking load situations, tensile stress is caused by the tipping action of a tooth during a 1-sided movement and is dramatically increased in the root (74 to 87 MPa versus 1 MPa during clenching).

As suggested in several other investigations,<sup>2,3,12</sup> for patients with heavy contacts, MZ100 is the preferable choice as it reduces tensile stress on ultrathin bonded posterior occlusal veneers. E.max CAD makes the underlying tooth less functional by not taking advantage of the tooth's natural ability to handle stress, resulting in greater tensile stress formation in the restoration. In practice, the clinician must also consider esthetics and wear of and from opposing teeth. From this perspective, the total wear (material and antagonist combined) seems to be more favorable for MZ100 than for ceramics.<sup>17</sup>

This simulation also emphasizes the need to reduce interferences by properly designing restorations to avoid high tensile stress located at the occlusal surface and root structure and to prevent possible root fracture. This simulation study is confirmed by the clinical results of Ratcliff et al,<sup>10</sup> showing that protecting teeth from excursive interferences and parafunction may prevent premature breakdown. Morphology, design, and load configuration (occlusion type) may all be instrumental in defining tensile stresses in addition to the nature of the restorative materials. Geometric change from convex versus concave surfaces influences tensile stress distribution<sup>18</sup> and causes high tensile stress concentration in occlusal fissures.<sup>11,16</sup> Enamel bridges and crests are thus needed to maintain restoration integrity under loading forces. The loading configuration of the veneers aimed to distribute the tensile stress using broad contacts with the antagonist. A small contact area will concentrate tensile stress and cause increased initial wear<sup>17</sup> for an already thin veneer.

Morphology dictates that tensile stress concentrates at geometric changes and surface irregularities. Hence, the challenge of designing restorations is to avoid these factors while maintaining morphological harmony and masticatory efficiency. The canines, not only because of their active guidance, passively position teeth into centric occlusion,<sup>19</sup> which tends to limit paraxial forces.

Clinical trials are currently under way<sup>9</sup> to compare the 2 materials tested in this study, using the occlusal veneer reconstruction concept. The clinical application of this technique is conservative and seems to be well tolerated by patients. It is, however, more technique sensitive and assumes that the clinician will undergo appropriate training.

## CONCLUSIONS

Based on the findings of this finite element simulation, the following conclusions were drawn:

1. Harmful effects were identified from occlusal interferences in terms of tensile stress in the restoration's occlusal topography and root structure.
2. The nonworking interference generated the highest tensile stresses in the restorations and should be

avoided by careful occlusal adjustments or by developing canine guidance.

3. Contact forces in working and nonworking movement cause significant tensile stress in the tooth root structure.

## REFERENCES

1. Lussi A, Jaeggi T. Erosion—diagnosis and risk factors. *Clin Oral Investig* 2008;12:5-13.
2. Magne P, Schlichting L, Maia H, Baratieri L. In vitro fatigue resistance of CAD/CAM composite resin and ceramic posterior occlusal veneers. *J Prosthet Dent* 2010;104:149-57.
3. Schlichting L, Maia H, Baratieri L, Magne P. Novel-design ultra-thin CAD/CAM composite resin and ceramic occlusal veneers for the treatment of severe dental erosion. *J Prosthet Dent* 2011;105:217-26.
4. Guess P, Schultheis S, Wolkewitz M, Zhang Y, Strub J. Influence of preparation design and ceramic thicknesses on fracture resistance and failure modes of premolar partial coverage restorations. *J Prosthet Dent* 2013;110:264-73.
5. Johnson A, Versluis A, Tantbirojn D, Ahuja S. Fracture strength of CAD/CAM composite and composite-ceramic occlusal veneers. *J Prosthodont Res* 2014;58:107-14.
6. Vailati F, Belser UC. Full-mouth adhesive rehabilitation of a severely eroded dentition: the three-step technique. Part 1. *Eur J Esthet Dent* 2008;3:30-44.
7. Vailati F, Belser UC. Full-mouth adhesive rehabilitation of a severely eroded dentition: the three-step technique. Part 2. *Eur J Esthet Dent* 2008;3:128-46.
8. Vailati F, Belser UC. Full-mouth adhesive rehabilitation of a severely eroded dentition: the three-step technique Part 3. *Eur J Esthet Dent* 2008;3:236-57.
9. Schlichting LH, Resende TH, Reis KR, Magne P. Simplified treatment of severe dental erosion with ultrathin CAD-CAM composite occlusal veneers and anterior bilaminar veneers. *J Prosthet Dent* 2016;116:474-82.
10. Ratcliff C, Becker IM, Quinn L. Type and incidence of cracks in posterior teeth. *J Prosthet Dent* 2001;86:168-72.
11. Magne P, Belser UC. Rationalization of shape and related stress distribution in posterior teeth: a finite element study using nonlinear contact analysis. *Int J Periodontics Restorative Dent* 2002;22:425-33.
12. Magne P, Stanley K, Schlichting L. Modeling of ultrathin occlusal veneers. *Dent Mater* 2012;28:777-82.
13. Magne P. Virtual prototyping of adhesively restored, endodontically treated molars. *J Prosthet Dent* 2010;103:343-51.
14. Waltimo A, Kononen M. A novel bite force recorder and maximal isometric bite force values for healthy young adults. *Scand J Dent Res* 1993;101:171-5.
15. Magne P, So W, Cascione D. Immediate dentin sealing supports delayed restoration placement. *J Prosthet Dent* 2007;98:166-74.
16. Magne P, Belser UC. Porcelain versus composite inlays/onlays: effects of mechanical loads on stress distribution, adhesion, and crown flexure. *Int J Periodontics Restorative Dent* 2003;23:543-55.
17. Kunzelmann KH, Jelen B, Mehl A, Hickel R. Wear evaluation of MZ100 compared to ceramic CAD/CAM materials. *Int J Comput Dent* 2001;4:171-84.
18. Magne P, Versluis A, Douglas W. Rationalization of incisor shape: experimental-numerical analysis. *J Prosthet Dent* 1999;81:345-55.
19. McAdam D. Tooth loading and cuspal guidance in canine and group-function occlusions. *J Prosthet Dent* 1976;35:283-90.

### Corresponding author:

Dr Pascal Christophe Magne  
 Department of Restorative Sciences, Herman Ostrow School of Dentistry of USC  
 University Park Campus  
 925 West 34th St, Room 4382  
 Los Angeles, CA 90089  
 Email: magne@usc.edu

### Acknowledgments

The authors thank Dr Francois Curnier (Digisens Inc) for providing the raw micro-CT data; and Dan Wolf (MSC Software) for helpful suggestions.

Copyright © 2016 by the Editorial Council for *The Journal of Prosthetic Dentistry*.